

Estimating Individual Treatment Effects using Non-Parametric Regression Models: a Review

Alberto Caron*

Department of Statistical Science
University College London

Ioanna Manolopoulou

Department of Statistical Science
University College London

Gianluca Baio

Department of Statistical Science
University College London

March 23, 2022

Abstract

Large observational data are increasingly available in disciplines such as health, economic and social sciences, where researchers are interested in causal questions rather than prediction. In this paper, we investigate the problem of estimating heterogeneous treatment effects using non-parametric regression-based methods. Firstly, we introduce the setup and the issues related to conducting causal inference with observational or non-fully randomized data, and how these issues can be tackled with the help of statistical learning tools. Then, we provide a review of state-of-the-art methods, with a particular focus on non-parametric modeling, and we cast them under a unifying taxonomy. After presenting a brief overview on the problem of model selection, we illustrate the performance of some of the methods on three different simulated studies and on a real world example to investigate the effect of participation in school meal programs on health indicators.

Keywords— Bayesian Non-Parametrics, Causal inference, Heterogeneous Treatment Effects, Machine Learning, Observational Studies, Regression Trees.

1 Introduction

The application of advanced statistical learning tools in causal inference has gained popularity in recent years, partly due to the fact that large datasets are becoming available at relatively lower costs (thanks to e.g. electronic health records, social network data etc.). One of the increasingly common objectives of causal inference in many disciplines is to draw inferences about individual-level treatment effects, as opposed to inferring treatment effects on average across the entire population. The importance of inferring individual-level treatment effects lies in the fact that treatment effects are very often heterogeneous across units of analysis. Two such examples arise in precision medicine and personalized

*Corresponding author: alberto.caron.19@ucl.ac.uk, 1-19 Torrington Pl, London WC1E 7HB.

advertisement, where the ultimate goal is to make decisions at the level of an individual patient or user. For instance, patients with high cholesterol levels respond differently to statin prescriptions based on their demographics. This level of analysis requires causal inference methods that can accurately predict the impact of treatment, as well as quantify its uncertainty, at a fine resolution. To this end, popular statistical learning algorithms that exhibit excellent predictive performance, such as tree ensembles, kernel methods and neural networks, can be exploited also, with due adjustments, in causal settings. This paper is therefore motivated by the growing number of non-parametric regression methods for modelling *Individual Treatment Effects* (ITE) using large datasets to answer individual-level questions, and reviews some of the most popular ones laying down the underlying assumptions and pros/cons for each of them.

Regardless of the precise causal questions of interest, the fundamental challenge in causal inference is that the quantity of interest — namely the effect of treatment — is an unknown model’s parameter. Moreover, treatment effect and selection into treatment are invariably entangled. As a result, advanced statistical learning tools, capable of exploiting large datasets in supervised learning settings, cannot be directly applied. Instead, the latent treatment effect is inferred by reconstructing counterfactual statements either through sampling (randomization in the administration of treatment) and/or by adjusting for covariates that affect both the outcome of interest and treatment assignment, and by doing so “confound” the treatment effect (confounding).

Randomized Controlled Trials (RCTs), where treatment is randomly allocated, marginally on confounding factors (such as medical or socio-economic characteristics), are considered to be the gold standard for causal inference. However, fully randomized studies are costly, difficult to access, and sometimes suffer from problems such as non-compliance and other issues of missingness not at random that might invalidate the randomization mechanism, or external validity of the results.

In contrast, data of observational nature, where treatment administration is not randomized, are more easily accessible and abundantly present in many applied fields. However, observational studies present several drawbacks, largely attributable to three complex phenomena. The first is *selection bias*, which manifests when the treatment allocation mechanism is not under the researcher’s control, but determined by observable or unobservable factors. This constitutes a potential source of confounding that needs to be controlled for, as it generates structural differences between the treated and the control groups. The second phenomenon is known as *partial overlap*, which occurs when there are regions in the space of relevant covariates where only treated, or only control, units are present. As a result, units in these particular regions lack an appropriate comparator with similar demographics. These two issues are closely related, as partial overlap may be a direct consequence of selection bias. The third phenomenon relates to the fact that treatment allocations and their corresponding outcomes may not be independent across individuals.

In this paper we review some of the most recent non-parametric regression methods for estimating heterogeneous effects arising from a binary treatment assignment, at a individual level, and introduce a taxonomy that classifies these methods under the same unified framework. More in details, we provide an overview of the implied assumptions and compare methods’ performance with the help of two simulated studies. In addition, we illustrate practical application of some of the methods on a real-world dataset to investigate the effect of participation to school meal programs on students’ health indicators, which is likely to display heterogeneity patterns depending on students’ demographics. We focus on methods which circumvent the potential issues stemming from lack of complete (and controlled) randomization by making a set of assumptions which are common in the literature. The first assumption is *unconfoundedness*, which ensures that there is no unobserved confounding factor driving selection into treatment. Unconfoundedness might be, in some cases, a strained assumption to make, but represents less of a threat in settings where a large number of relevant covariates is available.

The second assumption is *common support*, which states that each unit, identified by a given set of demographics, has non-zero probability of being observed in each of the treatment groups. In other words, common support ensures that there is no deterministic component in treatment administration. Finally, the last assumption is known as *Stable Unit Treatment Value Assumption* (SUTVA), and states that the response to treatment of one unit is not affected by other units' assignment to treatment, thus ensuring that there is no interference.

The rest of the work is organized as follows. Section 2 formulates the problem of estimating *Conditional Average Treatment Effect* (CATE) by using the potential outcomes representation by Rubin (1978). Section 3 reviews the most recent methods of estimating CATE and the problem of model selection. Section 4 presents results from two different simulated studies that we conducted to compare performance of some of the methods. Section 5 provides an example of a real-world social sciences application. Section 6 concludes with a discussion.

2 Problem setup

We will follow the Neyman-Rubin Causal Model, outlined in Rubin (1978) and Imbens and Rubin (2015), which conceives causal inference as a missing data problem. For each unit of analysis $i \in \{1, \dots, N\}$, given a binary treatment assignment $Z_i \in \{0, 1\}$, where $Z_i = 1$ indicates exposure to the treatment and $Z_i = 0$ indicates no exposure, the framework defines the quantities $(Y_i^{(0)}, Y_i^{(1)})$ as potential outcomes. $Y_i^{(1)}$ corresponds to unit i 's outcome under exposure to the treatment, while $Y_i^{(0)}$ corresponds to its outcome under no exposure, and only one of them is actually observed. We will consider, throughout this work, a setting where the outcome variable of interest is continuous, i.e., $(Y_i^{(0)}, Y_i^{(1)}) \in \mathbb{R}^2$, but most of the ideas and methods presented can be generalized. It is worth pointing out that the Neyman-Rubin framework is not the only viable approach to causal inference. For example, Dawid (2000) develops a critique of potential outcomes and proposes a different framework based on Bayesian decision analysis.

Given the framework outlined above, in case both potential outcomes were observed, one would have access also the *Individual Treatment Effects* (ITE), defined as $Y_i^{(1)} - Y_i^{(0)}$. However, as described earlier, the fundamental problem of causal inference is that, for each individual i , only one of the two potential outcomes $(Y_i^{(0)}, Y_i^{(1)}) \in \mathbb{R}^2$ is observed, corresponding to the realized treatment assignment: $Y_i = Z_i Y_i^{(1)} + (1 - Z_i) Y_i^{(0)}$. This implies that $Y_i^{(1)} - Y_i^{(0)}$ cannot be estimated as in a usual regression problem.

Given a dataset of either observational or randomized nature $\mathcal{D}_i = \{\mathbf{X}_i, Z_i, Y_i\}$, with $i \in \{1, \dots, N\}$, where $\mathbf{X}_i \in \mathcal{X}$ denotes a d -dimensional set of observed covariates for the individual i which are potential source of confounding to be controlled for, the aim is to estimate Conditional Average Treatment Effect (CATE), defined as

$$\tau(\mathbf{x}_i) = \mathbb{E}[Y_i^{(1)} - Y_i^{(0)} \mid \mathbf{X}_i = \mathbf{x}_i]. \quad (1)$$

The two quantities $\mu_Z(\mathbf{x}_i) = \mathbb{E}[Y^{(Z_i)} \mid \mathbf{X}_i = \mathbf{x}_i]$ in (1) are the conditional average potential outcomes. The intuition behind the estimation of $\tau(\mathbf{x}_i)$ is the following. In case both potential outcomes were observed, then $Y_i^{(1)} - Y_i^{(0)}$ (ITE) would be modelled as the response variable in a regression framework where \mathbf{X}_i are the d regressors, and where the aim is to estimate the conditional mean of the outcome, namely $\tau(\mathbf{x}_i) = \mathbb{E}[Y_i^{(1)} - Y_i^{(0)} \mid \mathbf{X}_i = \mathbf{x}_i]$. Figure 1 provides a graphical representation of a simple single-covariate example, where coloured dots show observed values $Y_i = Y^{(Z_i)}$ of the response, and grey their corresponding (unobservable) counterfactuals $Y_i^{(1-Z_i)}$. Notice that the example is purely illustrative and serves as visual aid to introduce the reader to the key concepts in the Rubin-Neyman

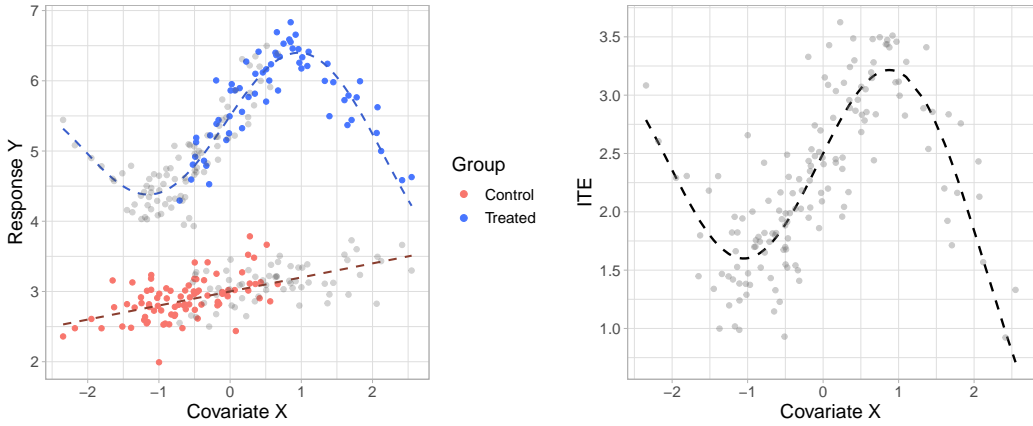


Figure 1: Simulated example with one single covariate X . Left panel: observed outcomes for the treated (blue dots) and control (red dots) groups with underlying conditional mean function (dashed lines), and unobservable counterfactual outcomes (grey dots). Right panel: unobservable true ITE (grey dots) and corresponding conditional mean function (dashed line).

framework.

An additional quantity of interest under the Neyman-Rubin framework is the *propensity score*, which is defined, for each unit of analysis i , as the probability of being selected into treatment, given a set of observed covariates that we denote by $\tilde{\mathbf{X}}_i = \tilde{\mathbf{x}}_i$, to stress the fact that it might be different from the set of covariates used for the estimation of $\tau(\mathbf{x}_i)$; more formally:

$$\pi(\mathbf{x}_i) = \mathbb{P}(Z_i = 1 \mid \tilde{\mathbf{X}}_i = \tilde{\mathbf{x}}_i) .$$

Thus, for each unit, the binary treatment assignment Z_i can be seen as the outcome of a Bernoulli experiment where $Z_i \sim \text{Bern}(\pi(\mathbf{x}_i))$. In the simple example of Figure 1, the propensity score is generated as a monotone function of the covariate X . This is why treated units are more frequently observed for higher values of X , while control units are more frequent for lower values of X . The propensity score distribution in this case is also slightly skewed to the right; as a consequence, there are more units in the control group compared to the treated one.

Under the potential outcomes framework, the untestable unconfoundedness assumption is equivalent to assuming the conditional independence

$$(Y_i^{(0)}, Y_i^{(1)}) \perp\!\!\!\perp Z_i \mid \mathbf{X}_i , \quad (2)$$

which ensures that selection is determined by observed demographics. A well-known result concerning the propensity score, derived by Rosenbaum and Rubin (1983), is that if (2) holds, then

$$(Y_i^{(0)}, Y_i^{(1)}) \perp\!\!\!\perp Z_i \mid \pi(\mathbf{X}_i) . \quad (3)$$

Conditional independence in (3) represents a different way of expressing unconfoundedness, by conditioning only on the propensity score rather than on the full set of covariates. In the context where the number of covariates is high, $\pi(\mathbf{X}_i)$ represents a 1-dimensional summary of a d -dimensional covariate set $\mathbf{X}_i \in \mathcal{X}$ which achieves conditional independence between outcome and treatment assignment. There are many different ways of making effective use of propensity score for deriving population-level or individual-level causal estimators. In some approaches propensity score assumes a central role, such

as in matching and blocking methods (Rosenbaum and Rubin, 1984, 1985), compared to regression-based methodologies that we focus on in this work. Imbens (2004) offers a nice and thorough overview of methods based on the propensity score, and also of other methods (e.g. regression and matching).

The assumption of common support, under the Rubin-Neyman framework, implies that propensity score is such that $0 < \pi(\mathbf{x}_i) < 1$, for each i , which equivalently means that treatment assignment is not deterministic, and that an individual with covariate values $\mathbf{X}_i = \mathbf{x}_i$ can be potentially observed in either treatment group with non-zero probability.

Under unconfoundedness and common support assumptions, CATE can be estimated from observed data in $\mathcal{D}_i = \{\mathbf{X}_i, Z_i, Y_i\} \ i \in \{1, \dots, N\}$. In fact, under unconfoundedness, the conditional average potential outcomes are such that

$$\begin{aligned} \mu_Z(\mathbf{x}_i) &= \mathbb{E} [Y^{(Z_i)} \mid \mathbf{X}_i = \mathbf{x}_i] = \mathbb{E} [Y^{(Z_i)} \mid Z_i = z_i, \mathbf{X}_i = \mathbf{x}_i] \\ &= \mathbb{E} [Y_i \mid Z_i = z_i, \mathbf{X}_i = \mathbf{x}_i] , \end{aligned} \quad (4)$$

for $z_i \in \{0, 1\}$, where the second equality generates from the conditional independence between $(Y_i^{(0)}, Y_i^{(1)})$ and Z_i given \mathbf{X}_i , while the last one from the identity $Y_i = Z_i Y_i^{(1)} + (1 - Z_i) Y_i^{(0)}$. Hence, as a straightforward implication of (4), one can derive an estimator for CATE as

$$\begin{aligned} \tau(\mathbf{x}_i) &= \mathbb{E} [Y_i^{(1)} - Y_i^{(0)} \mid \mathbf{X}_i = \mathbf{x}_i] \\ &= \mathbb{E} [Y_i^{(1)} \mid \mathbf{X}_i = \mathbf{x}_i] - \mathbb{E} [Y_i^{(0)} \mid \mathbf{X}_i = \mathbf{x}_i] \\ &= \mathbb{E} [Y_i^{(1)} \mid Z_i = 1, \mathbf{X}_i = \mathbf{x}_i] - \mathbb{E} [Y_i^{(0)} \mid Z_i = 0, \mathbf{X}_i = \mathbf{x}_i] \\ &= \mathbb{E} [Y_i \mid Z_i = 1, \mathbf{X}_i = \mathbf{x}_i] - \mathbb{E} [Y_i \mid Z_i = 0, \mathbf{X}_i = \mathbf{x}_i] , \end{aligned} \quad (5)$$

where, as in (4), the third equality is given by unconfoundedness, and the last one by the identity $Y_i = Z_i Y_i^{(1)} + (1 - Z_i) Y_i^{(0)}$. Common support assumption is then needed to guarantee that the two conditional average potential outcomes $\mu_Z(\mathbf{x}_i) = \mathbb{E} [Y^{(Z_i)} \mid \mathbf{X}_i = \mathbf{x}_i]$ exist for each values z_i and \mathbf{x}_i in their supports, and thus can be estimated through the observed quantities in the conditional expectations $\mathbb{E} [Y_i \mid Z_i = z_i, \mathbf{X}_i = \mathbf{x}_i]$. To clarify, suppose that common support does not hold for $\mathbf{X}_i = x^*$ and that $\pi(x^*) = 0$ (without loss of generality), then the conditional average potential outcome $\mu_1(x^*) = \mathbb{E} [Y^{(1)} \mid \mathbf{X}_i = x^*]$ does not theoretically exist, and it would not make sense to attempt to even estimate it.

2.1 Non-Parametric regression framework for CATE estimation

Throughout this work, we will review non-parametric regression approaches where the outcome surface Y_i is modelled as a function of (\mathbf{X}_i, Z_i) and some unobservable error term $\varepsilon_i : Y_i = g(\mathbf{X}_i, Z_i, \varepsilon_i)$. More specifically, the reviewed methods generally assume that the error term is additive and normally distributed, which leads to the following setup:

$$Y_i = f(\mathbf{X}_i, Z_i) + \varepsilon_i , \quad \text{where } \varepsilon_i \sim \mathcal{N}(0, \sigma^2) , \quad (6)$$

where $f(\mathbf{X}_i, Z_i) = \mathbb{E} [Y_i \mid \mathbf{X}_i, Z_i]$ is learnt from the data. The strength of non-parametric regression models is their robustness to misspecification of the functional form of $f(\cdot)$ (e.g. tree-based methods model $f(\cdot)$ as piece-wise constant, splines as piece-wise polynomial, etc.). The covariates $\mathbf{X}_i \in \mathcal{X}$ represent a potential source of confounding, in that they might affect both the treatment and the outcome, and are thus controlled for. In a setting where the number of available covariates is high,

one might want to resort to regularization in the estimation of $f(\cdot)$; this is more likely to be of interest in observational studies in socio-economic disciplines rather than clinical research, where closely controlling for which covariates are included in the model is preferable. However, as explained in both Hahn et al. (2018) and Hahn et al. (2020), regularization should be handled carefully in this context; we will return to this point in Section 3.1.6.

In the regression setup illustrated in (6), some of the methods reviewed in the next section reserve a specific role for the propensity score. For the remaining methods which do not explicitly use the propensity score, in the simulated studies that we conduct in Section 4, we follow the suggestion of Hahn et al. (2020) and incorporate it via the following two-stage regression framework:

$$\begin{aligned}\pi(\mathbf{X}_i) &= \mathbb{P}(Z_i = 1 \mid \mathbf{X}_i) \\ Y_i &= f([\mathbf{X}_i \ \pi(\mathbf{X}_i)], Z_i) + \varepsilon_i.\end{aligned}\tag{7}$$

The first stage in (7) involves estimating the propensity score, while the second embeds it as an extra covariate in the covariate set. Any probabilistic classifier is suitable for use in the first stage regression (e.g. logistic regression, probit Bayesian Additive Regression Trees, Gaussian Process Classifier, etc.). As explained in Hahn et al. (2020), and as we will describe later in Section 3.1.6, the addition of $\pi(\mathbf{X}_i)$ to the covariate set in (7) represents an effective way to tackle bias deriving from *targeted selection*. Targeted selection arises when individuals are selected into treatment based on the prediction of otherwise adverse outcome, i.e., when $\pi(\mathbf{X}_i)$ is a strictly monotone function of $\mathbb{E}[Y_i^{(0)} \mid \mathbf{X}_i = \mathbf{x}_i]$, and is common in many observational studies (e.g. medical or socio-economic studies).

CATE estimators can be derived from the representations in (6) and (7). There are a few different approaches for deriving an estimator for CATE from (6) and (7), that will be analyzed in the next section.

3 Estimating CATE

Given the framework outlined in the previous section, various meta-algorithms designed to derive a CATE estimator have been proposed in the literature. These meta-algorithms are often referred to as “Meta-Learners”, in that they are built on top of “base-learners”, which are common machine learning algorithms (e.g. tree ensembles, regularized regressions, neural networks etc.). We attempt to build a taxonomy of these “Meta-Learners” approaches in Section 3.1, while in Section 3.2 we present a review of the metrics used for model selection when estimating CATE, which is a substantially hard, arguably impossible, problem.

3.1 Meta-Learners

As mentioned in the earlier sections, we will partly build on top of the review of Künzel et al. (2019), and we will illustrate the most recent contributions stemming from both statistics and computer science literature. A concise summary of the presented “Meta-Learners”, together with the relevant references, can be found in Table 1.

3.1.1 S-Learners

“Single-Learners”, shortened to S-Learners, have been implicitly proposed in two early contributions (Hill, 2011; Foster et al., 2011) and derive an estimator for CATE by using treatment assignment as

Table 1: Summary of meta-learners described in this paper

	References	CATE estimator
S-Learner	Hill (2011); Foster et al. (2011)	$\tau(\mathbf{x}_i) = f(\mathbf{x}_i, 1) - f(\mathbf{x}_i, 0)$
T-Learner	Athey and Imbens (2016); Lu et al. (2018), Powers et al. (2018)	$\tau(\mathbf{x}_i) = f_1(\mathbf{x}_i) - f_0(\mathbf{x}_i)$
X-Learner	Künzel et al. (2019)	$\tau(\mathbf{x}_i) = \pi(\mathbf{x}_i)\tau_0(\mathbf{x}_i) + (1 - \pi(\mathbf{x}_i))\tau_1(\mathbf{x}_i)$
R-Learner	Nie and Wager (2019)	$\tau(\mathbf{x}_i) = \arg \min_{\tau} \left\{ L_n(\tau(\cdot)) + \Lambda_n(\tau(\cdot)) \right\}$
Multitask-Learner	Alaa and van der Schaar (2017, 2018)	$\tau(\mathbf{x}_i) = \mathbf{f}^\top(\mathbf{x}_i)\mathbf{e}$
τ-Learner	Hahn et al. (2020)	$\tau(\mathbf{x}_i)$ as explicit model parameter

“just another covariate” in the covariate space \mathcal{X} , which means that CATE is estimated as

$$\tau(\mathbf{x}_i) = f(\mathbf{x}_i, 1) - f(\mathbf{x}_i, 0). \quad (8)$$

An S-Learner fits a single surface $f(\cdot)$ through a base-learner and derives CATE estimates by taking the difference between the two conditional average potential outcomes, which are represented by the fitted $\hat{f}(\cdot)$ with $Z_i = 1$ and $Z_i = 0$ respectively. The underlying assumption is that the group-specific conditional average potential outcomes stem from the same model, with conditional mean function $f(\cdot)$ and error term ε_i . Regression trees are popular base-learners employed in the context of S-Learners. For instance, Hill (2011) advocates the use of Bayesian Additive Regression Trees (BART), while Foster et al. (2011) of random forests.

The left panel plot of Figure 2 shows a S-Learner BART fit for the conditional mean $\hat{f}(\cdot)$ of the single-covariate simulated example already encountered in Figure 1. Notice that the dashed line representing $\hat{f}(\cdot)$ has a unique color (grey) to emphasize the fact that S-Learner fits a unique surface.

Since a S-Learner fits a single regression, it is quite restrictive in the sense that it does not incorporate the way in which $f(\cdot)$ changes with respect to Z ; and it does not take into account the fact that the distribution of the covariates $\mathbf{X}_i \in \mathcal{X}$ may vary in Z , as a result of selection bias. This is obviously more problematic when working with observational data, while it is less so with randomized studies where selection bias is less likely to be present. Alaa and van der Schaar (2018) and Hahn et al. (2020) have both identified that the main drawback of S-Learners is their lack of ability in adapting to variable levels of sparsity and smoothness across the two treatment groups, since they impose the same regularizing conditions for both treated and control groups. A S-Learner will then perform poorly in a situation where the outcome surface complexity is very different across the two groups. On the contrary, S-Learner will perform well when CATE is of small magnitude, as $\tau(\mathbf{x}_i)$ surface complexity does not heavily depend on Z_i , or, in other words, does not vary much across treatment groups. For example, consider the case of a S-Learner employing a tree ensemble base-learner, such as BART. Since a tree ensemble method like BART picks splitting variables at each node in each tree randomly, it might not even choose Z as splitting variable in some of the trees in the ensemble, so that Z will possibly be included in most of the trees fitting the response Y , but not necessarily in all of them. The exclusion of Z from the splitting rules of a tree is more likely to happen as the number of covariates \mathbf{X}_i grows larger, in that the model has a larger set of splitting variables to pick from. This

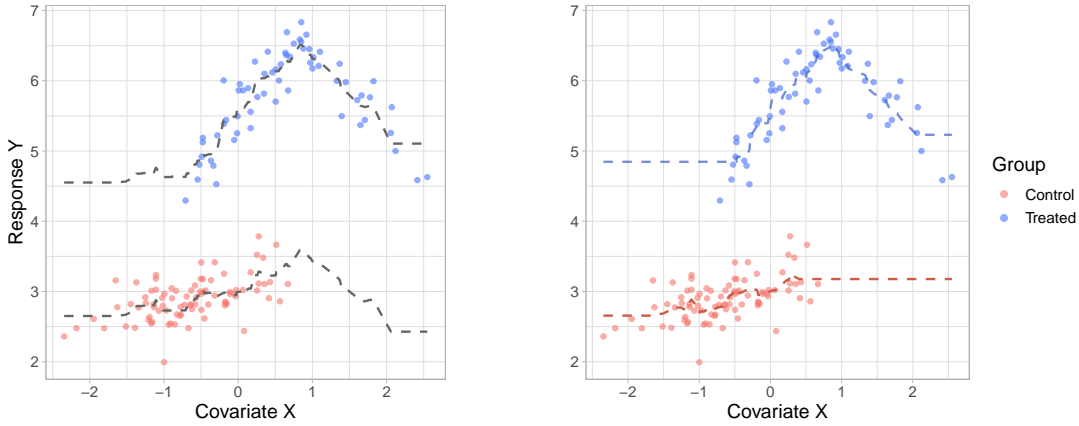


Figure 2: Simulated one-covariate data from Section 2. Left panel: conditional mean fit from a S-Learner BART (dashed grey line). Right panel: conditional mean fit from a T-Learner BART (blue and red dashed lines).

intuitively explains why S-Learners turn out to be appropriate in situations where the magnitude of ground-truth CATE is rather small, relative to the variation in outcome attributable to the covariates. It may happen in real world applications, e.g. in clinical studies, that the researcher has a prior idea regarding the magnitude of the treatment effect. As it becomes clearer in the following sections, this is a non-negligible piece of information when choosing a method to perform the analysis.

3.1.2 T-Learners

“Two-Learners”, shortened to T-Learners, derive an estimator for CATE by fitting two separate surfaces for the treated and control groups and computing their difference:

$$\tau(\mathbf{x}_i) = f_1(\mathbf{x}_i) - f_0(\mathbf{x}_i) . \quad (9)$$

Versions of T-Learners can be found in many contributions in the literature. For instance, Athey and Imbens (2016), Lu et al. (2018) and Powers et al. (2018) offer some examples employing decision trees, random forests and gradient boosted trees as base-learners respectively. In contrast to S-Learners, T-Learners separate the two treatment groups when modelling response variable Y , and assume that group-specific conditional average potential outcomes are derived from separate regression models, characterized by different conditional means $f_1(\cdot)$ and $f_0(\cdot)$ and independent error terms ε_{1i} and ε_{0i} . This allows to preserve distributional differences across the two groups that might originate from selection bias, and to take into account different degrees of sparsity and smoothness that vary with Z , when regressing Y against X . On the other hand, a shortcoming of T-Learners is that, as a result of splitting the sample in two, they do not allow sharing common underlying information between the groups when estimating the two surfaces. This is particularly not ideal in a scenario where individuals in the two groups share the same distributional characteristics, such as in a randomized study.

The right panel plot in Figure 2 displays a T-Learner BART fit for the conditional means of the two treatment groups $f_1(\cdot)$ and $f_0(\cdot)$, on the same one-covariate simulated example of Figure 1. Notice that fitted $\hat{f}_1(\cdot)$ and $\hat{f}_0(\cdot)$ are differentiated by colors (blue and red dashed lines respectively), emphasizing the fact that T-Learner fits two separate surfaces.

T-Learners work particularly well when complexity of the response surface is very different across

treatment groups, and so CATE itself turns out to be a rather complex function. In addition, as formally derived by Alaa and van der Schaar (2018), T-Learners are expected to do well as sample size N goes to infinity, and more observations per group are available to estimate $f_1(\cdot)$ and $f_0(\cdot)$. However, this is not usually the case with real world data. For example, in presence of imbalanced designs, where one group is larger than the other, splitting the sample in two would leave few observations for the estimation of f_Z in the smaller group. On the contrary, T-Learners tend to perform quite poorly in settings where CATE surface is relatively simple and heterogeneity patterns are not so sophisticated, i.e., situations where S-Learner usually performs better. Hence if subject-matter knowledge suggests that treatment impact is likely to be of significant magnitude, a T-Learner might be the preferred choice.

3.1.3 X-Learners

X-Learners have been proposed by Künzel et al. (2019) as an extension of T-Learners, and derive a CATE estimator in three steps. In the first step, conditional average potential outcomes are fitted as in a T-Learner approach, that is by using two separate regression models for the conditional means $f_1(\mathbf{x}_i)$ and $f_0(\mathbf{x}_i)$. This carries the same underlying assumptions, benefits and drawbacks of T-Learners, illustrated in the previous section. Then in the second step, “imputed treatment effects” are computed for each group separately; these are defined as the differences between the group-specific observed outcome Y_i^Z , and the estimated unobservable conditional average potential outcome $\hat{Y}_i^{(Z)}$ derived in the first step, more formally:

$$\begin{aligned}\tilde{D}_i^1 &= Y_i^1 - \hat{Y}_i^{(0)} && \text{if } Z_i = 1 \\ \tilde{D}_i^0 &= \hat{Y}_i^{(1)} - Y_i^0 && \text{if } Z_i = 0.\end{aligned}\tag{10}$$

The second step thus attempts to recover the unobservable differences $D_i = Y_i^{(1)} - Y_i^{(0)}$ (ITE) by replacing the unobservable potential outcomes with the relative conditional average potential outcome estimates $\hat{Y}_i^{(Z)}$, separately for the treated and control group. In the last step, \tilde{D}_i^1 and \tilde{D}_i^0 are used as response variables in two separate regressions, employing the chosen base-learner (linear regression, random forest, BART, etc.), to obtain estimates of $\hat{\tau}_1(\mathbf{x}_i)$ and $\hat{\tau}_0(\mathbf{x}_i)$, using covariates \mathbf{X}_i as regressors. These two independent regressions can be depicted as

$$\begin{aligned}\tilde{D}_i^1 &= \tau_1(\mathbf{X}_i) + \eta_{1i} && \text{if } Z_i = 1 \\ \tilde{D}_i^0 &= \tau_0(\mathbf{X}_i) + \eta_{0i} && \text{if } Z_i = 0,\end{aligned}\tag{11}$$

where the two estimated quantities $\hat{\tau}_1(\mathbf{x}_i)$ and $\hat{\tau}_0(\mathbf{x}_i)$ from (11) are group-specific CATE estimates. The final CATE estimate is then obtained through a weighted average of the two group-specific CATE estimates,

$$\hat{\tau}(\mathbf{x}_i) = g(\mathbf{x}_i)\hat{\tau}_0(\mathbf{x}_i) + (1 - g(\mathbf{x}_i))\hat{\tau}_1(\mathbf{x}_i),\tag{12}$$

where $g(\mathbf{x}_i) \in [0, 1]$ is a given weighting function. The authors propose to set $g(\cdot)$ equal to a propensity score estimate $g(\mathbf{x}_i) = \hat{\pi}(\mathbf{x}_i)$, but it can take different forms (e.g. $g(\mathbf{x}_i) = 1$ or $g(\mathbf{x}_i) = 0$).

The intuition behind the X-Learner approach is the following. If both potential outcomes were observable for each individual i , then $\mathbb{E}[Y_i^{(1)} - Y_i^{(0)} \mid \mathbf{X}_i = \mathbf{x}_i]$ (CATE) would be estimated by regressing $Y_i^{(1)} - Y_i^{(0)}$ (ITE) directly on the covariates \mathbf{X}_i . However, since the difference $Y_i^{(1)} - Y_i^{(0)}$ is not observable, one can estimate it by using the observed potential outcome Y_i^Z and replacing the counterfactual unobservable outcome $\hat{Y}_i^{(1-Z)}$ with an estimate, derived via T-Learner in the first step.

The procedure laid out by the X-Learner in the first two steps is comparable to that of a T-Learner

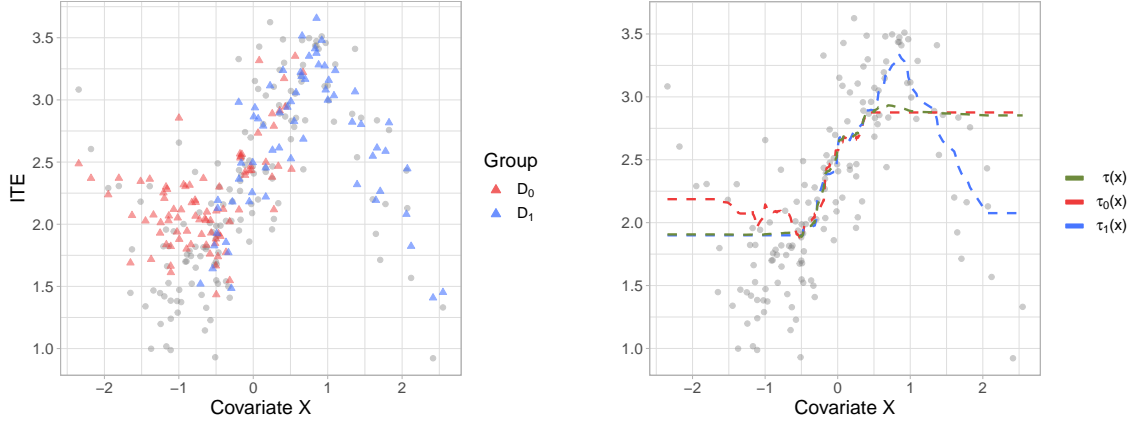


Figure 3: X-Learner BART applied to the simulated one-covariate example. Left panel: unobservable ITE (grey dots) and imputed treatment effects D^1 and D^0 (blue and red triangles), estimated as in (10) using T-Learner BART. Right panel: group-specific CATE estimates (blue and red dashed lines) obtained from the two regressions in (11), and final weighted CATE estimates (green dashed line) obtained from the re-balancing step in (12).

as both methods imply dividing the sample into the two groups. The main difference lies then in the last additional step, where the X-Learner attempts to re-balance CATE estimates through weighting via the estimated propensity score. X-Learners are in fact shown to perform well in unbalanced settings, where one of the treatment groups (typically the control group) is larger in size compared to the other one, and where T-Learner might face issues. A final note about the X-Learner balancing step is that it requires careful specification of the propensity score model, as poor PS estimates would defy the re-balancing purpose. Propensity score estimation is no different from a standard prediction problem and boils down to performing a probabilistic binary outcome regression of Z on \mathbf{X} . We will see that also other Meta-Learners envisage an important balancing role for propensity score, and thus must deal with its estimation.

Figure 3 offers a simple example of a X-Learner, with BART as base-learner, applied to the one-covariate simulated data encountered in Figure 1 and Figure 2. X-Learner's first step essentially derives, via T-Learner, the same BART estimates seen in the right panel plot of Figure 2. The output of the second step, namely the imputed treatment effects \tilde{D}_i^1 and \tilde{D}_i^0 , are depicted in the left panel plot of Figure 3 (red and blue triangles), together with the true ITE (grey dots). The graph on the right instead shows the estimated group-specific CATE $\hat{\tau}_1(\mathbf{x}_i)$ (blue dashed line) and $\hat{\tau}_0(\mathbf{x}_i)$ (red dashed line), derived from the two regressions in (11), and the final CATE estimate $\hat{\tau}(\mathbf{x}_i)$ (green dashed line), obtained from the weighting step in (12). Propensity score estimates employed for the weighting step were retrieved via probit version of BART. Notice that the final CATE estimates $\hat{\tau}(\mathbf{x}_i)$ lie in between the two fitted group-specific $\hat{\tau}_1(\mathbf{x}_i)$ and $\hat{\tau}_0(\mathbf{x}_i)$.

3.1.4 R-Learners

R-Learner was proposed by Nie and Wager (2019) as a two-stage meta-algorithm, which aims at minimizing a loss function, specifically defined on CATE, through parameter tuning. The derivation of the two-step procedure stems from Robinson (1988) decomposition of the outcome model in (6).

Define the following two quantities:

$$\begin{aligned} Y_i &= \mu(\mathbf{X}_i) + \tau(\mathbf{X}_i)Z_i + \varepsilon_i \\ m(\mathbf{X}_i) &= \mathbb{E}(Y_i \mid \mathbf{X}_i) = \mu(\mathbf{X}_i) + \tau(\mathbf{X}_i)\pi(\mathbf{X}_i) \end{aligned} \quad (13)$$

as the outcome model and the *conditional mean outcome* model, respectively. Under this setup, unconfoundedness assumption implies that the error term is such that $\mathbb{E}[\varepsilon_i \mid \mathbf{X}_i, Z_i] = 0$. Notice that under this parametrization $\tau(\mathbf{X}_i)$ (CATE) enters explicitly in the outcome regression model. By combining the two quantities above, Robinson (1988) noticed that the outcome model can be re-written as:

$$Y_i - m(\mathbf{X}_i) = (Z_i - \pi(\mathbf{X}_i))\tau(\mathbf{X}_i) + \varepsilon_i. \quad (14)$$

Starting from this decomposition, Nie and Wager (2019) derive a loss function that can be used for parameter tuning in the estimation of CATE; the optimal CATE estimates are defined as the minimizer of the following loss function:

$$\tau(\mathbf{X}_i) = \arg \min_{\tau} \left\{ \mathbb{E} \left[\left((Y_i - m(\mathbf{X}_i)) - (Z_i - \pi(\mathbf{X}_i))\tau(\mathbf{X}_i) \right)^2 \right] \right\}. \quad (15)$$

The idea is that a base-learner that relies heavily on parameter tuning (e.g. random forest or gradient boosted trees) can be tuned on the modified parametrization of the outcome model in (14), which includes a version of the outcome net of the impact of the covariates $m(\mathbf{X}_i)$ and propensity score balancing, instead of being tuned on the raw outcome Y_i as one would do in an S- or T-Learner procedure. Since we cannot observe directly the quantities in (15) for the minimization problem, the R-Learner overcomes the issue through the following two-step approach, i.e., by:

1. Fitting $\hat{m}(\mathbf{x}_i)$ and $\hat{\pi}(\mathbf{x}_i)$, by minimizing usual prediction error.
2. Plugging in estimates from the first step to estimate $\hat{\tau}(\mathbf{x}_i)$, by minimizing the regularized sample equivalent of (15), via cross-validation parameters tuning, that is:

$$\begin{aligned} \hat{\tau}(\mathbf{X}_i) &= \arg \min_{\tau} \left\{ \hat{L}_n(\hat{\tau}(\mathbf{X}_i)) + \Lambda_n(\hat{\tau}(\mathbf{X}_i)) \right\}, \quad \text{where} \\ \hat{L}_n(\hat{\tau}(\mathbf{X}_i)) &= \frac{1}{N} \sum_{i=1}^N \left((Y_i - \hat{m}^{-i}(\mathbf{X}_i)) - (Z_i - \hat{\pi}^{-i}(\mathbf{X}_i))\hat{\tau}(\mathbf{X}_i) \right)^2, \end{aligned} \quad (16)$$

and where $\Lambda_n(\hat{\tau}(\cdot))$ is a term representing regularization (e.g. Ridge or LASSO penalization, splines smoothness penalization, etc.), and the super-script $(-i)$ refers to the i -th observation being held-out from the estimation subsample, and used for leave-one out cross validation (LOO-CV).

The advantage of R-Learners lies in the fact that they take a two-stage procedure where the first step produces an estimate of propensity score $\hat{\pi}(\mathbf{x}_i)$, and by doing so mitigates confounding generated by the non-randomized selection mechanism. While in the second step, exploiting the parametrization in (13), they make use of a loss function through which parameters can be optimized to estimate $\hat{\tau}(\mathbf{x}_i)$ directly. R-Learners naturally work better with types of base-learners that rely heavily on parameter tuning, such as ensemble methods (e.g. gradient boosting, random forests, etc.).

3.1.5 Multitask-Learners

The idea of multitask-learning, or multi-output learning, for causal inference was introduced by Alaa and van der Schaar (2017) and Alaa and van der Schaar (2018), in the context of Gaussian Processes. The multitask perspective on CATE estimation consists in viewing the two potential outcomes $Y_i^{(0)}$ and $Y_i^{(1)}$ as output of a function $f : \mathcal{X} \rightarrow \mathbb{R}^2$, with d -dimensional input space and 2-dimensional output space, where the output space is indexed by Z_i , that acts as “task identifier”. CATE estimator is defined as the difference between the elements of the 2-dimensional output of $f(\cdot)$, i.e.,

$$\hat{\tau}(\mathbf{x}_i) = \hat{f}_1(\mathbf{x}_i) - \hat{f}_0(\mathbf{x}_i) = \hat{\mathbf{f}}^\top(\mathbf{x}_i)\boldsymbol{\xi}, \quad \text{where } \boldsymbol{\xi}^\top = [-1 \ 1]. \quad (17)$$

Equation (17) displays a very similar formulation to a T-Learner; and as in the T-Learner procedure, the sample is divided into the two subgroups for the estimation. However, the advantage of viewing CATE estimation as a multitask problem is that, instead of estimating the two potential outcomes independently as one would do in a T-Learner or X-Learner, they are estimated “jointly”, through the specification of some hyperparameters that trigger a joint optimization for the two “tasks”: learning $f_{Z=1}$ and $f_{Z=0}$. Hence, this approach fits separate conditional mean functions (as in a T-Learner), but at the same time attempts to recover common underlying patterns between the two groups (as in an S-Learner) that would be otherwise lost due to the sample split.

In the case of Alaa and van der Schaar (2017), multitask learning is induced through the specification of a particular structure in the stationary kernel function of the Gaussian Process prior. The method is labelled as *Causal Multitask Gaussian Process* (CMGP). Alaa and van der Schaar (2018) then proposed a similar method where multitask learning is induced via a non-stationary version of the GP kernel function (*Non-Stationary Gaussian Process* - NSGP). Both causal multitask GPs allow to compute posterior credible interval for CATE as natural result of their Bayesian approach.

Alaa and van der Schaar (2017) and Alaa and van der Schaar (2018) are two example of Multitask-Learners employing Gaussian Process regression as a base-learner, but there are different ways of inducing multitask learning using other types of base-learners (e.g. tree ensembles). Due to their similarity with T-Learners in deriving a CATE estimator, we expect Multitask-Learners to perform well when complexity of the response surfaces f_1, f_0 varies across groups, and CATE itself turns out to be a rather complex function.

3.1.6 τ -Learners

The last type of Meta-Learner presented in this work was developed by Hahn et al. (2020), under the name of “Bayesian Causal Forest”. The authors tackle the problem of CATE estimation with a Bayesian approach, where they exploit the same parametrization seen in the context of R-Learners. Particularly, they noticed that the parametrization

$$Y_i = \mu(\mathbf{X}_i) + \tau(\mathbf{X}_i)Z_i + \varepsilon_i, \quad (18)$$

can be viewed as a Bayesian regression framework where the *prognostic score*, defined as the impact of the covariates $\mathbf{X}_i \in \mathcal{X}$ on the outcome Y_i in absence of the treatment, $\mu(\mathbf{x}_i) = \mathbb{E}[Y_i | Z_i = 0, \mathbf{X}_i = \mathbf{x}_i]$, plays the role of the intercept, while $\tau(\mathbf{x}_i)$ the role of the slope. In this perspective, CATE is an explicit parameter of the model and thus can be treated in a Bayesian fashion through the specification of a prior distribution $p(\tau(\cdot))$, which can be shaped to convey prior knowledge and more targeted regularization that can capture even simple patterns of heterogeneity. Bayesian Causal Forest of Hahn et al. (2020) is composed by a pair of separate and independent BART priors placed on $\mu(\cdot)$ and $\tau(\cdot)$ respectively, but

the parametrization in (18) can be exploited using other Bayesian regression methods (e.g. Gaussian Process, Dirichlet Process regression, etc.).

In addition to the parametrization shown in (18), Hahn et al. (2020) make use of the two-stage procedure seen in (7), Section 2. The two-stage approach is motivated by the presence of a particular type of confounding, which the authors in Hahn et al. (2018) and Hahn et al. (2020) call *Regularization Induced Confounding* (RIC). The intuition behind RIC is the following: regularization applied directly on the two curves f_1, f_0 may have unintended consequences on the induced regularization on $\tau(\cdot)$, leading to biased estimates of CATE. RIC is shown to have a stronger effect when there is strong confounding, such as in presence of *targeted selection*, that is when individuals are selected into treatment based on the prediction of otherwise adverse outcome. Targeted selection implies a potential strictly monotone relationship between the propensity score $\pi(\mathbf{x}_i)$ and the prognostic score $\mu(\mathbf{x}_i) = \mathbb{E}[Y_i | \mathbf{X}_i, Z_i = 0]$, and is rather common in studies of observational nature. The proposed way to tackle confounding from targeted selection is precisely to use the two-stage representation illustrated in (7), where a probabilistic estimate of the propensity score $\hat{\pi}(\mathbf{x}_i)$, obtained from the first stage regression, is added to the covariates for the estimation of $\mu(\mathbf{x}_i) = \mathbb{E}[Y_i | \mathbf{X}_i, Z_i = 0]$ in the second stage, to account for their potential relationship.

We name the above approach τ -Learner, as it involves an explicit parametrization in terms of $\tau(\mathbf{x}_i)$ and a direct Bayesian approach to CATE estimation. Hahn et al. (2020) specifically make use of BART for estimation of $\mu(\mathbf{x}_i)$ and $\tau(\mathbf{x}_i)$, but any other Bayesian method could potentially work. As a further advantage, the direct Bayesian approach allows to obtain valid posterior credible intervals for CATE.

3.2 Model Selection

Model selection is a challenging problem in causal inference. The main reason is that researchers cannot access counterfactual outcomes $Y_i^{(1-Z_i)}$ and thus observe the difference $Y_i^{(1)} - Y_i^{(0)}$, $\forall i \in \{1, \dots, N\}$, which distinguishes it from other classical model selection problems. The aim here is to select a model $\mathcal{M}^* \in \{\mathcal{M}_1, \dots, \mathcal{M}_d\}$, which minimizes a loss function of the estimated CATE $\hat{\tau}$. We will review some of the methods that have been proposed, partly following the review in Schuler et al. (2018).

Standard likelihood-based criteria such as AIC and BIC are doomed to fail in a structural missing data context such as the one depicted. Other popular metrics in the ML literature might be used, such as prediction error in estimating the two conditional average potential outcomes $\mu_{z_i}(\mathbf{x}_i) = \mathbb{E}[Y_i | \mathbf{X}_i = \mathbf{x}_i, Z_i = z_i]$, that are the expression of the two surfaces $f_1(\cdot)$ and $f_0(\cdot)$, that is

$$\hat{\mathbb{E}}_\mu[\ell(\hat{\mu}_z, \mu_z)] = \frac{1}{N} \sum_{i=1}^N \left(\hat{\mu}_{z_i}(\mathbf{x}_i) - y_i^{(z_i)} \right)^2. \quad (19)$$

A slightly modified version of (19) takes into account the observational nature of the data at hand and uses inverse propensity score estimates for weighting the prediction error in estimating each μ_z , that is,

$$\hat{\mathbb{E}}_{\mu, IPTW}[\ell(\hat{\mu}_z, \mu_z)] = \frac{1}{N} \sum_{i=1}^N \frac{(\hat{\mu}_{z_i}(\mathbf{x}_i) - y_i^{(z_i)})^2}{\hat{\pi}_{z_i}(\mathbf{x}_i)}. \quad (20)$$

The main reason why these metrics work poorly is that they do not express a direct loss function on CATE. CATE squared-loss function, of the type $\ell(\hat{\tau}, \tau) = \mathbb{E}[(\hat{\tau} - \tau)^2]$, was defined as *Precision in Estimating Heterogeneous Treatment Effects* (PEHE) by Hill (2011) and takes the following form:

$$\mathbb{E}[(\hat{\tau}_i - \tau_i)^2 | \mathbf{X}_i = \mathbf{x}_i]. \quad (21)$$

PEHE would be the ideal loss function to use, but cannot be computed since one of the two potential outcomes is unobservable. Attempts have been made in the literature to render the estimation of PEHE feasible, through plug-in estimates of τ_i , but understandably none of them has been successful and commonly used so far. These approaches generally propose to use a Meta-Learner to estimate CATE on a portion of training sample N_{train} , then to derive CATE estimates also on a portion of held-out validation sample N_{val} (where $N = N_{train} + N_{val}$). The training set CATE estimates, denoted by $\tilde{\tau}(\mathbf{x}_i)$, will act as the ground-truth CATE, while the validation set estimates, denoted by $\hat{\tau}(\mathbf{x}_i)$, are instead used to validate the model. Given these two quantities, an estimator of PEHE is constructed as

$$\hat{\mathbb{E}}_\tau[\ell(\hat{\tau}, \tau)] = \frac{1}{N_{val}} \sum_{i=1}^{N_{val}} (\hat{\tau}(\mathbf{x}_i) - \tilde{\tau}(\mathbf{x}_i))^2. \quad (22)$$

A slightly different version of (22) replaces the training set estimate of CATE $\tilde{\tau}(\mathbf{x}_i)$ with a version of the observed outcome y_i weighted by the inverse propensity score, to correct for selection bias typically found in observational studies, and reads:

$$\hat{\mathbb{E}}_{\tau, IPTW}[\ell(\hat{\tau}, \tau)] = \frac{1}{N_{val}} \sum_{i=1}^{N_{val}} \left(\hat{\tau}(\mathbf{x}_i) - \frac{(2z_i - 1)y_i}{\tilde{\pi}_{z_i}(\mathbf{x}_i)} \right)^2, \quad (23)$$

where $\tilde{\pi}_{z_i}(\mathbf{x}_i)$ is a propensity score estimate obtained on the training set N_{train} . The advantage of this version is that instead of employing the training set CATE estimate $\tilde{\tau}(\mathbf{x}_i)$ as ground-truth, it replaces it with $\frac{(2z_i - 1)y_i}{\tilde{\pi}_{z_i}(\mathbf{x}_i)}$, which contains observed y_i and z_i , and an estimate of the propensity score that can be obtained through supervised approaches.

However, the evident setback of these plug-in methods is that they exhibit high model-dependent bias, which derives from the fact that the plug-in estimates of the ground-truth CATE $\tilde{\tau}(\mathbf{x}_i)$ (or those of the propensity score) obtained on a training subset of the data, clearly depend on the method used for the estimation. In this way $\hat{\mathbb{E}}_\tau[\ell(\hat{\tau}, \tau)]$ actually measures the error of $\hat{\tau}(\mathbf{x}_i)$ in estimating the training set CATE $\tilde{\tau}(\mathbf{x}_i)$, rather than in estimating the ground-truth CATE $\tau(\mathbf{x}_i)$.

Finally, it is worth noticing that the R-Learner presented in the previous section develops an actual loss function for $\tau(\cdot)$ in (16). However this can be exploited exclusively in the context of R-Learners (e.g. comparing a random forest R-Learner with a BART R-Learner), as it implies assuming Robinson (1988) parametrization as in (13).

4 Simulation studies

In this section we report and comment on results from two different semi-simulated studies, carried out to compare performance of some of the models presented above in estimating CATE. A third supplemental semi-simulated study can be found in the Appendix Section A. A semi-simulated study consists in simulating only the outcome surface Y_i in the tuple $\mathcal{D}_i = \{\mathbf{X}_i, Z_i, Y_i\}$, starting from real-world \mathbf{X}_i and Z_i . In the case of observational semi-simulations, Hill (2011) introduced a practical way of recreating an observational study from a randomized one. This is essentially done by leaving out a non-random portion of the treated group, so that treatment assignment is no longer random. Recreating an observational study from a purely randomized one has the main advantage of allowing control over the selection mechanism and that the common support assumption holds for the treated group.

We provide results based on the analysis of two real world randomized controlled trials, after transforming them into observational studies. The first semi-simulated setup employs the IHDP dataset,

Table 2: Tested models

Family	Name	Description
Linear Models	S-OLS	Linear regression as S-Learner
	T-OLS	Linear regression as T-Learner
	R-LASSO	LASSO regression as R-Learner
Naive Non-Parametrics	k NN	k -Nearest Neighbors
Tree-Based Methods	CF	Causal Forest
	S-BART	BART as S-Learner
	T-BART	BART as T-Learner
	BCF	Bayesian Causal Forest
Gaussian Processes	R-BOOST	Gradient Boosting as R-Learner
	CMGP	Causal Multi-task Gaussian Process
	NSGP	Non-Stationary Gaussian Process

firstly introduced by Hill (2011) and popular in both the computer science and statistics literature on CATE estimation. The second and third setups instead employ the ACTG-175 dataset, available in the R package `speff2trial`, and differ in the way the outcome and ITE are generated. Both datasets are publicly available. As mentioned above, we present here below results from the IHDP data simulation and one of the two setups involving the ACTG-175 data, while we leave the other ACTG-175 setup in the Appendix Section A.

The models tested include: linear regressions with S-Learner and T-Learner approach respectively (S-OLS and T-OLS); a penalized LASSO regression, through which we induce variable selection, with R-Learner approach (R-LASSO); a simple non parametric k -Nearest Neighbors (k NN) as T-Learner; a Causal Forest (CF), proposed by Wager and Athey (2018) as a modified version of Random Forests, where after partitioning the sample space on the covariates X , the last split in each tree in the ensemble is made on Z ; Bayesian Additive Regression Trees as S-Learner and T-Learner respectively (S-BART and T-BART); a Bayesian Causal Forest (BCF), i.e., a τ -Learner; Gradient Boosted trees with R-Learner procedure (R-BOOST); and finally the two causal multitask versions of Gaussian Processes, one with stationary kernel (CMGP) and the other with non-stationary kernel (NSGP), developed by Alaa and van der Schaar (2017) and Alaa and van der Schaar (2018) respectively. A summary of the tested models is provided in Table 2 below.

For each of the two datasets analyzed, in order to provide a comparison of the methods presented above, we computed $\sqrt{\text{PEHE}}$ estimates for each of the $B = 1000$ Monte Carlo simulations, and we averaged it over all the simulations. Estimates of PEHE were obtained through its sample equivalent, namely:

$$\widehat{\text{PEHE}}_{\tau} = \frac{1}{N} \sum_{i=1}^N \left(\tau(\mathbf{x}_i) - \widehat{\tau}(\mathbf{x}_i) \right)^2, \quad (24)$$

where $\widehat{\tau}(\mathbf{x}_i)$ is the CATE estimate obtained under the given method, while $\tau(\mathbf{x}_i)$ is the ground-truth CATE, which is always unknown in the real world, but in this case is simulated. Data are randomly split in 70% train set used to train the models, and 30% test set to evaluate the model on unseen data. $\sqrt{\text{PEHE}}$ is reported for both train and test data.

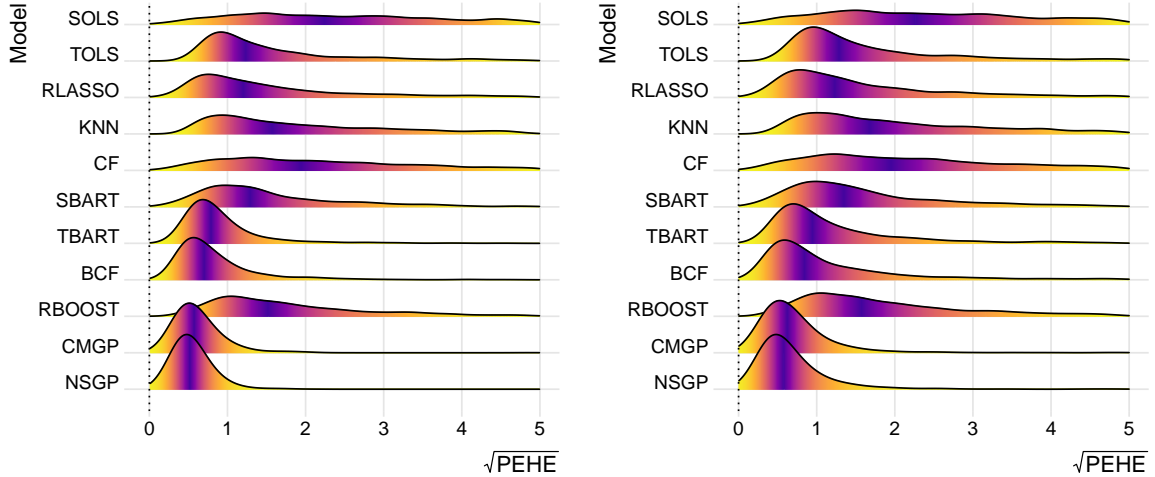


Figure 4: $\sqrt{\text{PEHE}}$ distribution on train set (left) and test set (right), IHDP data.

4.1 IHDP data

The first semi-simulated setup makes use of the IHDP dataset, popular in the literature for CATE estimation and used for the first time in Hill (2011). It includes data taken from the Infant Health and Development Program (IHDP), a randomized controlled trial carried out in 1985, aimed at improving health and cognitive status of premature infants with low weight at birth, through follow-ups and parent support groups. The dataset includes 25 covariates, 6 continuous and 19 binary. The data are transformed into observational by leaving out a non-random portion of the treated individuals, namely those with non-white mothers. This leaves 139 observations in the treated group and 608 in the control group, for a total of 747 observations.

ITE is derived as the difference between the simulated potential outcomes, which are generated as:

$$\begin{aligned} Y^{(0)} &\sim \mathcal{N}\left(\exp((X + W)\beta_B), 1\right), \\ Y^{(1)} &\sim \mathcal{N}(X\beta_B - \omega_B^b, 1), \end{aligned} \quad (25)$$

where W is an offset matrix of same dimension as X with every entry equal to 0.5, and β_B is a 25-dimensional vector of regression coefficients $(0, 0.1, 0.2, 0.3, 0.4)$, sampled with probabilities $(0.6, 0.1, 0.1, 0.1, 0.1)$ (“Response surface B” in Hill (2011)). For each simulation $b \in \{1, \dots, 1000\}$, ω_B^b is an offset chosen to guarantee that the population-level “Average Treatment effect on the Treated” (ATT) is equal to $ATT = \mathbb{E}[Y^{(1)} - Y^{(0)} | Z = 1] = 4$.

Simulation results are reported in Table 3 and Figure 4. The best models appear to be the multitask Gaussian Processes (CMGP and NSGP) of Alaa and van der Schaar (2017) and Alaa and van der Schaar (2018). This does not come as unexpected for two reasons related to the way the potential outcomes are simulated. First, the simulated setting tends to accommodate Meta-Learners fitting separate surfaces f_1, f_0 (T-Learners, X-Learners, Multitask-Learners), since the two simulated potential outcomes display very different degrees of complexity. Indeed, T-Learners in Table 3 show better performance than their S-Learner counterparts (e.g. T-BART vs S-BART). The second reason is that potential outcomes generated in (25) are rather smooth, and Gaussian Process regression tends to adapt well to non-linear continuous surfaces. We report also, in Figure 4, the distribution of $\sqrt{\text{PEHE}_\tau}$ over the $B = 1000$ iterations on both train and test data, for each of the models. We also notice that

Table 3: IHDP and ACTG-175 data. $\sqrt{\text{PEHE}_\tau}$ estimates \pm 95% confidence intervals for each tested model, on the train and test sets respectively.

	IHDP		ACTG-175	
	Train	Test	Train	Test
S-OLS	4.78 \pm 0.32	4.78 \pm 0.32	0.299 \pm 0.003	0.300 \pm 0.003
T-OLS	1.94 \pm 0.13	2.02 \pm 0.13	0.591 \pm 0.007	0.601 \pm 0.008
R-LASSO	1.99 \pm 0.15	2.05 \pm 0.16	0.309 \pm 0.006	0.310 \pm 0.006
<i>k</i> NN	2.67 \pm 0.19	2.98 \pm 0.21	0.903 \pm 0.004	0.902 \pm 0.005
CF	3.71 \pm 0.25	3.68 \pm 0.25	0.292 \pm 0.004	0.291 \pm 0.004
S-BART	1.93 \pm 0.13	2.06 \pm 0.14	0.298 \pm 0.003	0.299 \pm 0.003
T-BART	0.94 \pm 0.04	1.41 \pm 0.09	0.530 \pm 0.005	0.530 \pm 0.006
BCF	0.88 \pm 0.05	1.34 \pm 0.10	0.281 \pm 0.003	0.282 \pm 0.003
R-BOOST	2.28 \pm 0.14	2.48 \pm 0.16	0.408 \pm 0.006	0.405 \pm 0.006
CMGP	0.64 \pm 0.04	0.76 \pm 0.06	0.354 \pm 0.009	0.346 \pm 0.008
NSGP	0.55 \pm 0.02	0.71 \pm 0.05	0.293 \pm 0.003	0.292 \pm 0.003

tree-based methods are relatively more prone to overfitting.

An important remark about the data generating process described by (25) is that it does not really induce strong confounding, since it is easy for a non-parametric base-learner to distinguish the two underlying polynomials $\mathbb{E}[Y^{(Z_i)} | \mathbf{X}_i = \mathbf{x}_i]$. Besides, the fact that noise around the conditional mean is independently simulated for the two potential outcomes produces extra noise around CATE that often results in unrealistically large variation in the simulated ITE. In the ACTG-175 simulated example illustrated in Section 4.2, we will follow the parametrization found in Nie and Wager (2019) and Hahn et al. (2020) in the data generating process of the outcome surface, in order to induce stronger confounding (which is believed to be common in observational studies) and avoid creating unnecessarily high noise around CATE.

4.2 ACTG-175 data

The second semi-simulated setup presented here is created using ACTG 175 clinical trial data, freely available in the R package `speff2trial`. The data come from a randomized placebo-controlled trial aimed at comparing monotherapy versus a combination of therapies in HIV-1-infected subjects with CD4 cell counts between 200 and 500 (Hammer et al. (1996) for details). As in the case of IHDP data, an observational study is recreated by throwing away a non-random subset of patients, namely those not showing symptomatic HIV infection. The final dataset consists of 813 observations and 12 variables (3 continuous and 9 binary). We simulate continuous outcome and treatment effects by trying to resemble sign and magnitude of the estimated treatment effect fitted with a simple linear model, and also the scale of the original outcome (CD4 cell counts, on a log scale). Variables included in the dataset are shown in Table 4.

Unlike the case of IHDP data, response surface Y_i is not generated via simulation of the two potential outcomes. Instead, we generate continuous outcome Y_i according to the parametrization

$$Y_i = \mu(\mathbf{X}_i) + \tau(\mathbf{X}_i)Z_i + \varepsilon_i , \quad (26)$$

which allows to specify CATE directly, instead of starting from the simulation of potential outcomes, and to induce more confounding through the prognostic score function $\mu(\mathbf{x}_i)$. The prognostic score

Table 4: ACTG 175 data variables

Variable	Description
<i>age</i>	Numeric
<i>wtkg</i>	Numeric
<i>hemo</i>	Binary (hemophilia = 1)
<i>homo</i>	Binary (homosexual = 1)
<i>drugs</i>	Binary (intravenous drug use = 1)
<i>oprior</i>	Binary (non-zidovudine antiretroviral therapy prior to initiation of study treatment = 1)
<i>z30</i>	Binary (zidovudine use in the 30 days prior to treatment initiation = 1)
<i>preanti</i>	Numeric (number of days of previously received antiretroviral therapy)
<i>race</i>	Binary
<i>gender</i>	Binary
<i>str2</i>	Binary: antiretroviral history (0 = naive, 1 = experienced)
<i>karnof_hi</i>	Binary: Karnofsky score (0 = < 100, 1 = 100)

$\mu(\mathbf{x}_i)$ and CATE $\tau(\mathbf{x}_i)$ are generated as:

$$\begin{aligned}
 \mu(\mathbf{x}_i) = & 8 - 0.07hemo - 0.002|wtkg - 1| + 0.06gender - \frac{0.1}{age + 2} \\
 & + 0.007karnof_hi - 0.1z30 - 0.05race \\
 \tau(\mathbf{x}_i) = & 0.1 + 0.1age \cdot (karnof_hi + 2) .
 \end{aligned} \tag{27}$$

Then noise is added by simulating normally distributed errors $\varepsilon_i \sim \mathcal{N}(0, \sigma^2)$, with standard deviation equal to $\sigma = (\mu_{max} - \mu_{min})/2$, where μ_{max} is the maximum value of the generated prognostic score across the sample, that is $\mu_{max} = \{\mu(x_j) : \mu(x_j) > \mu(\mathbf{x}_i), \forall i \in \{1, \dots, N\} \setminus \{j\}\}$, while μ_{min} is the minimum. Notice that, unlike the case of IHDP data, the error term is not simulated independently for the two groups, which avoids imposing too much noise around CATE. This translates into generally lower and less variable estimated PEHE for all models compared to the case of IHDP data, as shown both in Table 3 and Figure 5.

In this simulated setting CATE is of rather simple and known form. Hence, we expect S-Learner to outperform their T-Learner counterparts. Indeed, this is exactly what Table 3 shows. S-Learners all display lower $\sqrt{\text{PEHE}}$ than T- and Multitask-Learners, with the only exception of NSGP, which instead performs quite well. BCF turns out to be the best method in this scenario, thanks to its ability to adjust to stronger confounding and apply more regularization when learning CATE, which allows to capture small and weakly heterogeneous treatment effect patterns. Figure 5 depicts again the distribution of $\sqrt{\text{PEHE}}$ over the $B = 1000$ simulations, for both train and test data, for all the tested models.

We employ ACTG-175 data also in a third semi-simulated setup featuring more complex $\mu(\mathbf{x}_i)$ and $\tau(\mathbf{x}_i)$ surfaces, compared to the ones in (27). Description and results of this third example are provided in the Appendix Section A.

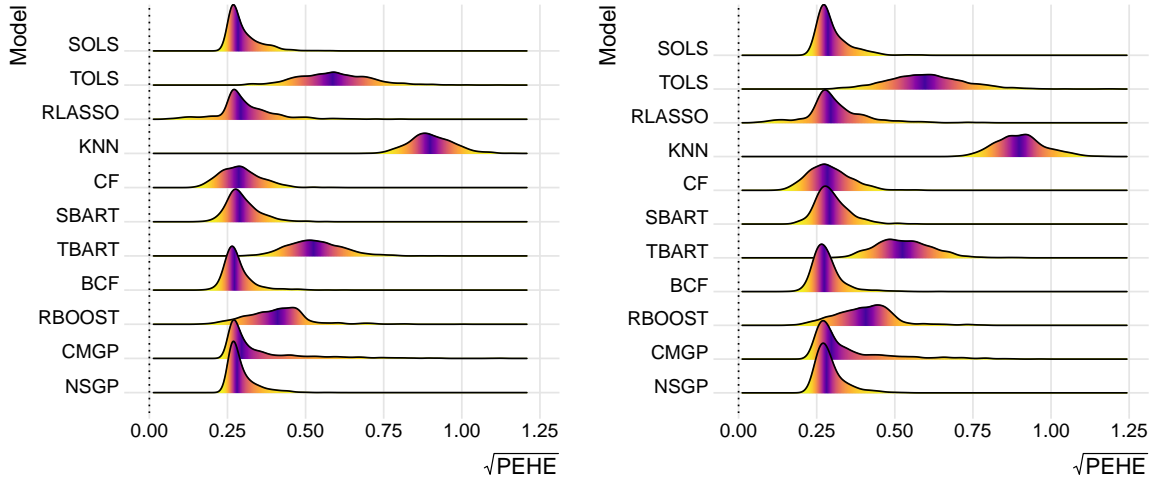


Figure 5: $\sqrt{\text{PEHE}}$ distribution on train set (left) and test set (right), ACTG-175 data.

5 The effect of school meal programs on health indicators

Social, economic and political sciences are among the disciplines that rarely benefit from RCTs studies, and often have to rely on observational or non-fully randomized data to address causal questions. In this section we provide an example of a real world social sciences application of the models reviewed in previous sections, to demonstrate their usefulness in applied research. To this end, we make use of the `nhanes_bmi` dataset found in the `ATE` R package. The dataset consists in a subset of the 2007-2008 National Health and Nutrition Examination Survey (NHANES), containing the variables shown in Table 5. The data are employed in this context to investigate whether participation to school meal programs is associated to improved children’s health indicators. There is reason to believe that the impact of such programs is heterogeneous across individuals, in that demographics such as age, gender or ethnicity are likely to play a role in how effective participation is (e.g. younger kids might benefit more than older ones, etc.). This supports the use of methods for individual treatment effects estimation.

Contrary to a simulated study, in a real world application it is impossible to recognize the type of heterogeneity patterns one encounters. For this reason, it is usually good practice to deploy more than just a single model to estimate CATE. In this specific context, we derive and compare CATE estimates from both Bayesian Causal Forest (BCF) and non-stationary Multitask Gaussian Process (NSGP), as from the simulation studies they emerged to be the most flexible methods when it comes to adapt to different types of surfaces.

We find that CATE estimates obtained from the two models are highly correlated, with Pearson’s and Spearman’s coefficients equal to 0.93 and 0.92 respectively, but BCF exhibits higher variance in the estimates (sample standard deviation of 0.09) compared to NSGP (sample standard deviation of 0.03). This means that BCF estimates capture much more heterogeneity. The left panel plot of Figure 6 depicts the densities of CATE estimates derived from each model, and NSGP’s estimates appear to be far more concentrated around the mean and generally indicate larger impact. The main source of the difference in dispersion between the two obtained estimates is likely to be child’s age covariate. As illustrated in the right panel plot in Figure 6, BCF attributes higher degree of treatment heterogeneity to child’s age compared to NSGP, although they both indicate slightly non-linear monotone relationship between the two quantities.

Table 5: NHANES data variables

Variable	Description
<i>BMI</i>	Numeric. Body mass index (outcome variable)
<i>school_meal</i>	Binary (treatment indicator)
<i>age</i>	Numeric (child's age)
<i>childSex</i>	Binary (male = 1)
<i>afam</i>	Binary (African American = 1)
<i>hisam</i>	Binary (Hispanic = 1)
<i>povlev_200</i>	Binary (family above 200% federal poverty lvl = 1)
<i>sup_nutr</i>	Binary (supplementary nutrition program = 1)
<i>stamp_prog</i>	Binary (food stamp program = 1)
<i>food_sec</i>	Binary (food security in household = 1)
<i>ins</i>	Binary (any insurance = 1)
<i>refsex</i>	Binary (adult respondent gender is male = 1)
<i>refage</i>	Numeric (adult respondent's age)

The impossibility of directly measuring performance of the methods prevents from carrying out proper model selection, as outlined in details in Section 3.2. However, it appears that both models support the existence of treatment heterogeneity, although with different patterns. In particular, BCF detects a stronger moderating effect of child's age on treatment effect than NSGP, while to other covariates (such as gender and ethnicity) the two methods attribute very similar moderating effects.

6 Conclusion

In the previous sections, we covered the most recent developments on the estimation of heterogeneous treatment effect in the context of non-randomized studies. We use here the phrase “non-randomized” studies as the methods illustrated are well suited for observational studies, but also for RCTs that might display threats to randomization such as imperfect compliance and non-random missingness (obviously also pure RCTs, sample size permitting).

Our review and simulation studies lead to a few general observations. A first simple but practical suggestion in applied setting where CATE is to be estimated, is to implement more than just one single method, to provide robustness to the results, given that it is impossible to discern which particular scenario the researcher faces (weak vs strong heterogeneity, simple vs complex CATE patterns, etc.). Secondly, it is clear from the semi-simulated exercises that non-parametric regression methods adapt well to non-linearities, and in general to complexity of the CATE function, whereas parametric ones are naturally less robust to functional form misspecification, unless heterogeneity patterns are very weak (reverting to homogeneity). In addition, Bayesian approaches to non-parametric modelling sacrifice some computational cost for less cumbersome parameter tuning and nicer posterior properties (i.e., posterior credible interval).

A final remark concerns τ -learners, and BCF in particular. Bayesian Causal Forest of Hahn et al. (2020) appears to show nice adaptability and robustness to misspecification regarding the CATE surface (i.e., smoothness, sparsity, heterogeneity vs homogeneity of treatment effect) compared to other Meta-Learners examined. This ability stems directly from the explicit inclusion of $\tau(\mathbf{x}_i)$ as a “parameter” in a regression framework, which is designed specifically to detect moderating impact of the covariates on treatment effects, and allows to place a direct prior distribution in a Bayesian fashion. From an empirical perspective, this implies some degree of flexibility in the choice of $p(\tau(\mathbf{x}_i))$. In fact,

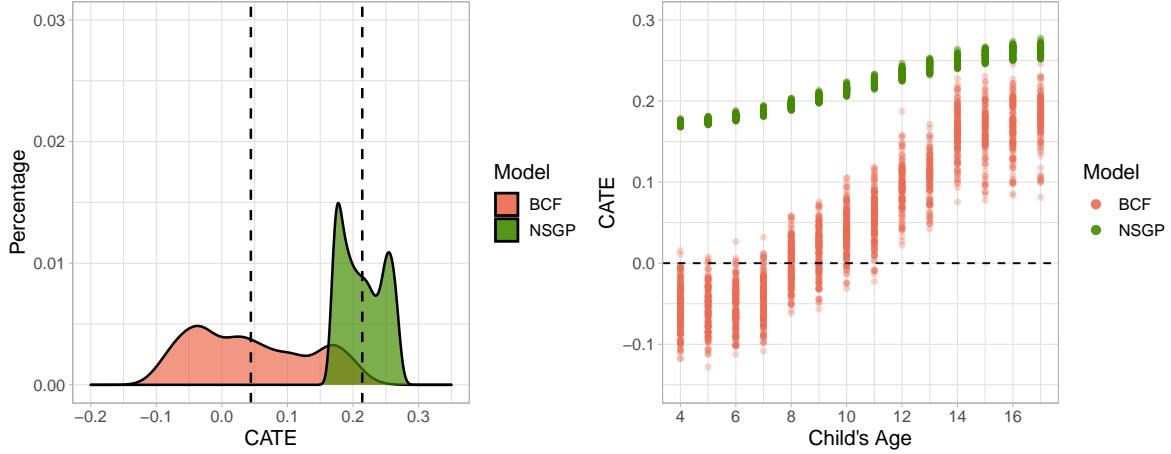


Figure 6: Left panel: kernel density of CATE estimates from the two models (dashed lines are the sample means). Right panel: CATE estimates from the two models as a function of child’s age.

the prior on $\tau(\mathbf{x}_i)$ can translate into a more or less targeted regularization based on prior knowledge on the complexity of CATE surface. In a case where CATE is believed to be complex one might, for example, modify default options to have deeper trees in the estimation of τ . On the contrary, in case little or no a priori knowledge is possessed, a more agnostic prior, which prevents overfitting via stronger regularization and leaves some degree of freedom in CATE estimation, can be chosen. This is something extraneous to the other methods found in the literature that, although the promising performances (the “causal” Gaussian Processes, CMGP and NSGP, in particular), do not allow to treat CATE as a model parameter and to specify of a prior distribution on it, thus not allowing to convey a priori knowledge, which is frequently of interest in causal analysis.

References

Alaa, A. and M. van der Schaar (2018). Limits of estimating heterogeneous treatment effects: Guidelines for practical algorithm design. In *Proc. 35th Inter. Conf. on Mach. Learn*, Volume 80, pp. 129–138.

Alaa, A. M. and M. van der Schaar (2017). Bayesian inference of individualized treatment effects using multi-task Gaussian Processes. pp. 3427–3435.

Angrist, J. D., G. W. Imbens, and D. B. Rubin (1996). Identification of causal effects using instrumental variables. *J. Am. Stat. Assoc.* 91, 444–455.

Athey, S. and G. Imbens (2016). Recursive partitioning for heterogeneous causal effects. 113, 7353–7360.

Chipman, H. A., E. I. George, and R. E. McCulloch (1998). Bayesian CART model search. *J. Am. Stat. Assoc.* 93, 935–948.

Chipman, H. A., E. I. George, and R. E. McCulloch (2010). BART: Bayesian additive regression trees. *Ann. Appl. Stat.* 4, 266–298.

Dawid, A. P. (2000). Causal inference without counterfactuals. *J. Am. Stat. Assoc.* 95, 407–424.

Foster, J. C., J. m. G. Taylor, and S. J. Ruberg (2011). Subgroup identification from randomized clinical trial data. *Stat. Med.* 30 24, 2867–80.

Hahn, P. R., C. M. Carvalho, D. Puelz, and J. He (2018). Regularization and confounding in linear regression for treatment effect estimation. *Bayesian Anal.* 13, 163–182.

Hahn, P. R., J. S. Murray, and C. M. Carvalho (2020). Bayesian regression tree models for causal inference: Regularization, confounding, and heterogeneous effects. *Bayesian Anal.*.

Hammer, S. M., D. A. Katzenstein, M. D. Hughes, H. Gundacker, R. T. Schooley, R. H. Haubrich, W. K. Henry, M. M. Lederman, J. P. Phair, M. Niu, M. S. Hirsch, and T. C. Merigan (1996). A trial comparing nucleoside monotherapy with combination therapy in hiv-infected adults with CD4 cell counts from 200 to 500 per cubic millimeter. *N. Engl. J. Med.* 335, 1081–1090.

Hartford, J., G. Lewis, K. Leyton-Brown, and M. Taddy (2017). Deep IV: A flexible approach for counterfactual prediction. In *Proc. 34th Inter. Conf. on Mach. Learn.*, Volume 70, pp. 1414–1423.

Hastie, T., R. Tibshirani, and J. Friedman (2001). *The Elements of Statistical Learning*. New York: Springer.

Heckman, J. J. (1979). Sample selection bias as a specification error. *Econometrica* 47, 153–161.

Hill, J. L. (2011). Bayesian nonparametric modeling for causal inference. *J. Comput. Graph. Stat.* 20, 217–240.

Hudgens, M. G. and M. E. Halloran (2008). Toward causal inference with interference. *J. Am. Stat. Assoc.* 103, 832–842.

Imbens, G. W. (2004). Nonparametric estimation of average treatment effects under exogeneity: A review. *Rev. Econ. Stat.* 86, 4–29.

Imbens, G. W. and D. B. Rubin (2015). *Causal Inference for Statistics, Social, and Biomedical Sciences: An Introduction*. Cambridge: Cambridge University Press.

Johansson, F. D., U. Shalit, and D. Sontag (2016). Learning representations for counterfactual inference.

King, G. and R. Nielsen (2019). Why propensity scores should not be used for matching. *Political Anal.*.

Künzel, S. R., J. S. Sekhon, P. J. Bickel, and B. Yu (2019). Metalearners for estimating heterogeneous treatment effects using machine learning. *J. Am. Stat. Assoc.* 116, 4156–4165.

Linero, A. R. (2018). Bayesian regression trees for high-dimensional prediction and variable selection. *J. Am. Stat. Assoc.* 113, 626–636.

Lu, M., S. Sadiq, D. J. Feaster, and H. Ishwaran (2018). Estimating individual treatment effect in observational data using random forest methods. *J. Comput. Graph. Stat.* 27, 209–219.

Morris, T. P., I. R. White, and M. J. Crowther (2019). Using simulation studies to evaluate statistical methods. *Stat. Med.* 38, 2074–2102.

Nie, X. and S. Wager (2019). Quasi-oracle estimation of heterogeneous treatment effects.

Pearl, J. (2018). Theoretical impediments to machine learning with seven sparks from the causal revolution. pp. 3.

Powers, S., J. Qian, K. Jung, A. Schuler, N. H. Shah, T. Hastie, and R. Tibshirani (2018). Some methods for heterogeneous treatment effect estimation in high dimensions. *Stat. Med.* 37, 1767–1787.

Robinson, P. M. (1988). Root-N-Consistent semiparametric regression. *Econometrica* 56, 931–954.

Rosenbaum, P. R. and D. B. Rubin (1983). The central role of the propensity score in observational studies for causal effects. *Biometrika* 70, 41–55.

Rosenbaum, P. R. and D. B. Rubin (1984). Reducing bias in observational studies using subclassification on the propensity score. *J. Am. Stat. Assoc.* 79, 516–524.

Rosenbaum, P. R. and D. B. Rubin (1985). Constructing a control group using multivariate matched sampling methods that incorporate the propensity score. *Am. Stat.* 39, 33–38.

Rubin, D. B. (1978). Bayesian inference for causal effects: The role of randomization. *Ann. Statist.* 6, 34–58.

Schuler, A., M. Baiocchi, R. Tibshirani, and N. Shah (2018). A comparison of methods for model selection when estimating individual treatment effects.

Starling, J., J. Murray, P. Lohr, A. Aiken, C. Carvalho, and J. Scott (2019). Targeted Smooth Bayesian Causal Forests: An analysis of heterogeneous treatment effects for simultaneous versus interval medical abortion regimens over gestation.

Tchetgen, E. and T. VanderWeele (2010). On causal inference in the presence of interference. *Stat. Methods Med. Res.* 21, 55–75.

Wager, S. and S. Athey (2018). Estimation and inference of heterogeneous treatment effects using random forests. *J. Am. Stat. Assoc.* 113, 1228–1242.

Yao, L., S. Li, Y. Li, M. Huai, J. Gao, and A. Zhang (2018). Representation learning for treatment effect estimation from observational data. In *Adv. Neural Inf. Process Syst.* 31, pp. 2633–2643.

A ACTG-175 data: third simulated exercise

In this short appendix section we present results obtained from a third semi-simulated exercise involving the ACTG-175 dataset. The structure of the utilized ACTG-175 data is exactly the same as the one found in the other example (same number of covariates and sample size). The difference lies in how the prognostic score and CATE functions are simulated. For this third setup we chose slightly more complex surfaces compared to the ones in the other ACTG-175 simulation, to provide an additional example on the performance of the reviewed methods under a more challenging data generating process (closer to the one seen in the IHDP data example). More specifically, the two $\mu(\mathbf{x}_i)$ and $\tau(\mathbf{x}_i)$ surfaces are generated as

$$\begin{aligned}\mu(\mathbf{x}_i) &= 6 + 0.3wtkg^2 - \sin(age) \cdot (gender + 1) + 0.6hemo \cdot race - 0.2z30 , \\ \tau(\mathbf{x}_i) &= 1 + 1.5 \sin(wtkg) \cdot (karnofhi + 1) + 0.4age^2 .\end{aligned}\tag{28}$$

Surfaces in (28) feature more complex functions and more interaction terms. As in the other ACTG-175 data setup, Gaussian noise was added by simulating $\varepsilon_i \sim \mathcal{N}(0, \sigma^2)$, with standard deviation equal to $\sigma = (\mu_{max} - \mu_{min})/10$, where μ_{max} is the maximum value of the generated prognostic score across the sample, while μ_{min} is the minimum value.

Table 6: Third simulated setup (ACTG-175 data). $\sqrt{\text{PEHE}_\tau}$ estimates \pm 95% confidence intervals for each tested model, on the train and test sets respectively.

ACTG-175: 3 rd surface		
	Train	Test
S-OLS	1.67 \pm 0.01	1.67 \pm 0.01
T-OLS	1.27 \pm 0.01	1.31 \pm 0.01
R-LASSO	1.29 \pm 0.01	1.31 \pm 0.01
<i>k</i> NN	1.17 \pm 0.01	1.19 \pm 0.01
CF	0.98 \pm 0.01	0.98 \pm 0.01
S-BART	0.98 \pm 0.01	0.99 \pm 0.01
T-BART	0.91 \pm 0.01	0.93 \pm 0.01
BCF	0.79 \pm 0.01	0.83 \pm 0.01
R-BOOST	0.95 \pm 0.01	0.96 \pm 0.01
CMGP	0.58 \pm 0.01	0.61 \pm 0.01
NSGP	0.56 \pm 0.01	0.59 \pm 0.01

Results in terms of performance of the tested models are reported in Table 6. A ranking similar to the one encountered in the IHDP data example emerges, with the GP Multitask-Learners being the best methods, followed up by BCF. This is explained by the fact that CATE here is the result of a complex function, which tends to favour methods that fit separate surfaces (T-Learners, Multitask-Learners, etc.), just like in the IHDP example. Notice in fact that also in this case T-Learners show better performance than their S-Learner counterparts (T-OLS vs S-OLS, T-BART vs S-BART).